Chapter 4

Pure and Nanocomposite Thin Films Based on TiO_2 Prepared by Sol-Gel Process: Characterization and Applications

Nelcy Della Santina Mohallem,
Marcelo Machado Viana,
Magnum Augusto Moraes Lopes de Jesus,
Gustavo Henrique de Magalhães Gomes,
Luiz Fernando de Sousa Lima and
Ellen Denise Lopes Alves

Additional information is available at the end of the chapter

http://dx.doi.org/10.5772/intechopen.74335

Abstract

Titanium dioxide (TiO_2) thin films have innumerable applications, and the preparation of nanocomposites based on TiO_2 favors the coupling of different structures that can lead to additional or enhanced properties. The aim of this chapter is to show the preparation and characterization of TiO_2 thin films and some nanocomposites based on anatase-TiO_2, prepared by sol-gel process using the dip-coating technique. TiO_2 thin films were prepared by sol-gel process onto borosilicate glass, steel, magnet, and silicon substrates from alcoholic starting solutions containing titanium isopropoxide, isopropyl alcohol, and acids to the control of the velocity of gelation. The doped thin films, such as SiO_2/TiO_2, Ag/TiO_2, and Nb/TiO_2, were prepared adding the dopants in a form of salts or alkoxides in starting solution. The morphological, structural, and textural characterization of the films was made using X-ray diffraction (XRD), high resolution transmission electron microscopy with energy-dispersive spectrometer (EDS) detector, atomic force microscopy/nanoindentation, and UV-Vis spectroscopy. Photoelectrical, mechanical, biological, optical, and surface properties were evaluated.

Keywords: TiO_2 thin films, Ag/TiO_2, Nb/TiO_2, SiO_2/TiO_2

1. Introduction

Titanium dioxide (TiO_2) is a multifunctional, semiconductor and polymorphic material, which is commercialized in rutile or anatase phases, both in tetragonal crystal structures. TiO_2 is used in industry since 1918 as pigment in paints, paper, plastic, drugs, cosmetics, etc. In the last years, with the beginning of nanotechnology, powder and films of titanium dioxide have been widely studied due to its new properties obtained by decreasing the particles size. The wide range of application is due to its electronic and structural properties, such as high transmittance in the visible, high refractive index (n = 2.6), high photocatalytic activity, and chemical stability. These properties make TiO_2 an excellent material for use in photocatalysis, antimicrobial surfaces, self-cleaning and hydrophobic surfaces, photovoltaic cells, gas sensor, photochromic devices, etc. [1].

Titanium is the second transition metal on the periodic table and has Ar-$3d^2 4s^2$ distribution. It was discovered in 1791 by the mineralogist William Gregor, in the region of Cornwall, United Kingdom, in the mineral ilmenite ($FeTiO_3$). In 1795, it was isolated by the German chemist Heinrich Klaproth in the form of TiO_2 rutile phase. Titanium dioxide can be found in three different crystalline phases: anatase, brookite, and rutile. By thermal treatment, it is possible to convert the anatase and brookite phases in rutile, which is thermodynamically stable at high temperatures. The anatase phase is more reactive, mainly in nanometric dimension, and is frequently used in photocatalytic applications.

As semiconductor, TiO_2 can be studied in terms of the energy band theory, whose bandgap energy (3.2–3.6 eV) can be supplied by photons with energy in the near ultraviolet range and whose separation between valence and conduction bands is intrinsically linked with its optical and electronic properties. These bandgap values depend on the particle size, phase, and used dopant, making possible the modulation of these values. In the case of thin films, which traditionally are formed by TiO_2 nanoparticles, the thickness also contributes to the modulation of the bandgap values. Several studies are made aiming the best quality of the films and the decrease in the bandgap energy by introduction of dopants in the TiO_2 structures to improve the photocatalytic propriety in the visible region of the light [1, 2].

The introduction of dopants in the TiO_2 thin film structure such as SiO_2, Ag, and Nb, among others, changes its properties expanding the range of possible applications. The methods of preparation also influence significantly its morphology, structure, and texture, modifying its properties. Several methods can be used to obtain thin films such as chemical vapor deposition, sputtering, spray pyrolysis, and sol-gel process. The sol-gel process [3] allows the preparation of thin films with high purity, thermal and mechanical resistance, chemical durability and the control of morphology, composition, thickness, and porosity. Thin film depositions using the sol-gel process can be realized by dip-coating, spin-coating, or spray-coating techniques. These techniques are economically feasible and can be applied to substrates with large surfaces and different forms.

1.1. Sol-gel process

The sol-gel process [3] that leads to the formation of TiO_2 films is based on mechanisms of hydrolysis and polycondensation of titanium alkoxides mixed with alcohol and catalytic agents. There are various kinds of Ti alkoxides such as titanium isopropoxide ($Ti(O^iPr)_4$) and

http://dx.doi.org/10.5772/intechopen.74335

titanium ethoxide ($Ti_4(OEt)_{16}$), among others, that need to be used preferentially with their correspondent alcohol. The precursor solution, also called sol, is a colloidal suspension of Ti surrounded by ligands, with physical-chemical properties adequate to the formation of a film. After a deposition, which can be by dip-coating, spin-coating, and spray-coating processes, the film is formed by a wet gel that became a dry gel after drying process. The hydrolysis of the alkoxide group to form Ti—OH occurs due to nucleophilic substitution of O—R groups (alkyl group) by hydroxyl groups (—OH) and the condensation of the group Ti—OH, to produce Ti—O—Ti and by-products (H_2O and ROH), leading to formation of the gel, according to the equation below:

$$Ti(OR)_n + nH_2O \rightarrow Ti(OH)_n + nROH \quad (1)$$

$$Ti(OH)_n \rightarrow Ti(O_{n/2}) + n/2\ H_2O \quad (2)$$

$$TiOR + TiOH \rightarrow TiO_2 + ROH \quad (3)$$

This mechanism is relatively complex because the reactions occur simultaneously during the process of deposition. In this proposed mechanism, the alkoxide precursor passes by the sequences, oligomer, polymer, and colloid, and it finishes as an amorphous porous solid structure. Thermal treatments are used for the preparation of nanocrystalline thin films. With the use of doping salts in the precursor solutions, the mechanism becomes more complex due to the introduction of other metals in the gel network.

The dip-coating technique [4] consists into dip a substrate in the sol and removes it at constant speed (**Figure 1**), resulting in an M—O—M oxide network that forms a wet gel film. The network structure, the morphology, and the thickness of the film depend on the contributions of the reactions of hydrolysis and condensation that must occur in approximately the same velocity of substrate withdrawal. Otherwise, the solution may run down the substrate. These properties may be controlled varying the experimental conditions: type of organic binder, the molecular structure of the precursor, water/alkoxide ratio, type of catalyst and solvent,

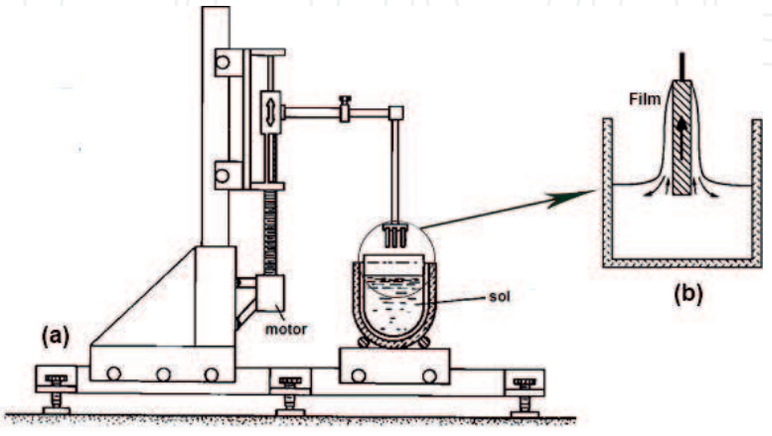

Figure 1. (a) Dip-coating equipment and (b) substrate withdrawal of the solution for film formation.

withdrawal speed, and solution viscosity. After the deposition, the gel film is formed by a solid structure impregnated with the solvent, and a drying process can be used to convert the wet gel in a dry porous film. Denser film can be tailored by different temperatures of thermal treatment, leading to films with different specific surface areas and porosities.

The advantage of the dip-coating process is the ease of deposition in substrates of any size and shape, facilitating the industrial process.

2. TiO_2 thin films

2.1. Experimental

TiO_2 thin films were prepared by sol-gel process [2, 5] using titanium isopropoxide (Aldrich, 98%) as the precursor of titania mixed with isopropyl alcohol and hydrochloric acid in stoichiometric amounts. The precursor solution was kept under agitation at room temperature for 1 h and rested until the viscosity reaches the best value condition, between 2 and 5 cP. The films were prepared using solutions with $2 < pH < 4$ and atmosphere relative humidity <40%, since they are opaque and not adherent for other pH and relative humidity values. The films were deposited onto clean substrates (borosilicate glass, steel, silicon, and magnets) at room conditions (25°C, relative air humidity lower than 30%), using a dip-coating equipment with withdrawal speed between 0.2 and 1.5 mm/s. The substrates were washed with standard cleaning method before dipping. After each dip-coating process, the wet films were dried in air for 30 min and thermally treated at temperatures between 100 and 500°C for a range of time (between 10 and 60 min) to convert them into porous or densified oxide films. Depending on the thermal treatment temperature, the films can be amorphous or nanocrystalline. Some samples were submitted at UV-C light (lamp Girardi RSE20B, 254 nm—15 W) to crystallize without increasing the temperature. Crystalline structures were investigated by an X-ray diffraction (incidence angle of 5°) using a diffractometer Rigaku (Geigerflex model 3034). The samples were analyzed by atomic force microscopy (AFM) in an Asylum Research, model MFP-3D-SA, to observe the topography and possible coating defects, such as cracks and peeling. Morphological characterization was evaluated by transmission electron microscopy (FEI TECNAI G2 20 at acceleration tension of 200 kV). Electron diffraction was also used to determine the structure of the crystalline phases. The films were pulled from glass substrates and mounted onto 200 mesh copper grids coated with holey carbon films for examination. The morphology and composition were evaluated by a scanning electron microscope (SEM) FEI Quanta 200 FEG with an energy-dispersive spectrometer (EDS). The transparency and thickness of the films deposited on glasses were verified by the optical transmission spectra measured with an ultraviolet and visible spectrometer (U3010, Hitachi).

2.2. Results

The TiO_2 films obtained by sol-gel process using the dip-coating technique are transparent, homogeneous, adherent, durable, and free of micro-cracks. **Figure 2a** shows thin films removed

http://dx.doi.org/10.5772/intechopen.74335

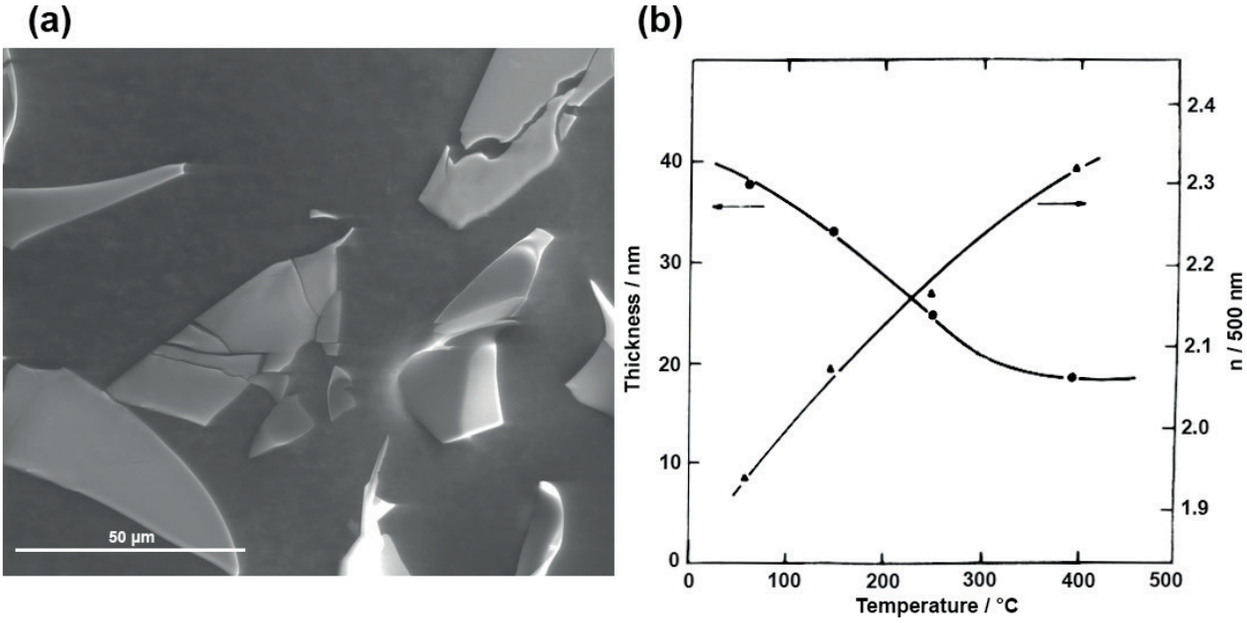

Figure 2. (a) TiO_2 thin films removed from a glass substrate and (b) thickness and refractive index of TiO_2 thin films in function of thermal treatment temperature.

from a glass substrate. The thickness of the films deposited in glass and dried in air can range from 40 to 800 nm for each coating, depending on the withdrawal speed and viscosity. After heating, the film thickness decreases due to the densification process, reaching values between 20 and 300 nm each coating. When the number of coating increased, the thickness can reach 800 nm after calcination without cracks.

After drying, the films are porous when treated at low temperatures, and the density increases as a function of heating temperature and time. The porosity of the films leads to a variation in the refraction index that can change from 1.9 to 2.3 (λ = 550 nm) for porosities between 20 and 5%, respectively. **Figure 2b** shows an example of the variation of thickness and refractive index in the function of thermal treatment temperature of TiO_2 film. When the TiO_2 films are deposited in substrates that cannot be thermally treated, such as polymers and cotton, the densification and crystallization can be made by UV light treatment. **Figure 3** shows images of TiO_2 films heated at 100 and 400°C for 10 min.

The film formed after drying at room temperature is amorphous and contains organic contaminants in the network. With increasing in temperature of thermal treatment, the film structure changes to anatase phase around ~300°C and to rutile phase above ~600°C.

According to the literature, the values of the phase transition of TiO_2 can change in some degrees also depending on the type and time of drying, used dopant, and particle size, among others factors. **Figure 4** shows typical diffractograms of TiO_2 films deposited in glass substrate in two temperatures, generating an amorphous material at 100°C and a nanocrystalline material at 400°C. **Figure 5** shows SEM and TEM images of the film and the respective electron diffraction that confirm its anatase phase.

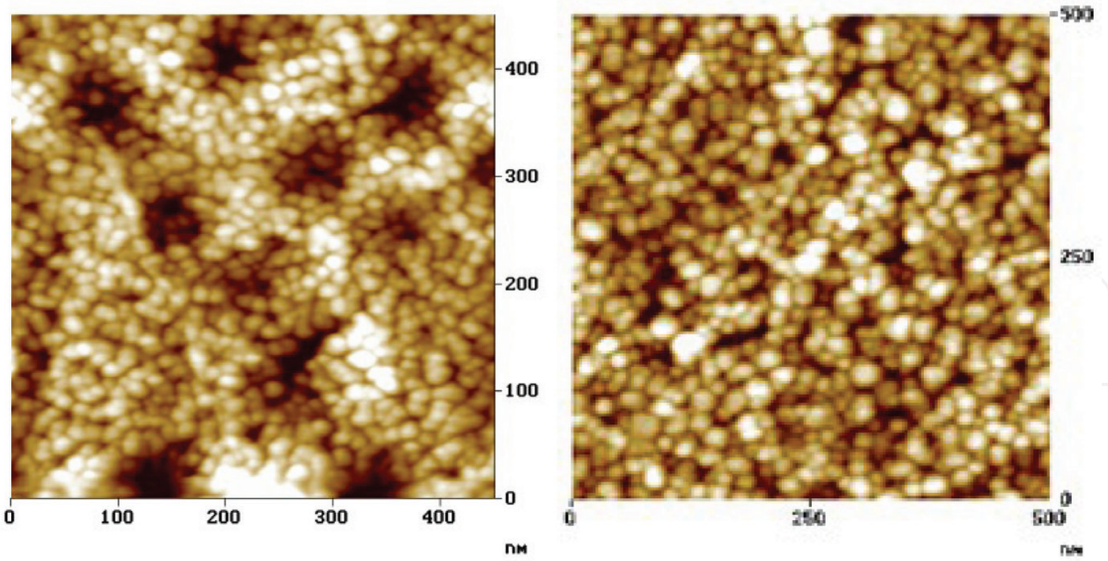

Figure 3. Atomic force microscopy of TiO_2 films heated at (a) 100°C and (b) 400°C.

TiO_2 thin films are used in the confection of optical devices (linear and nonlinear) due to the transparency throughout the visible spectrum, high linear and nonlinear refractive index that change in function of the wavelength, and dielectric properties. Their nonlinearity can make possible operations such as logic, all-optical switching, and wavelength conversion. Their high linear index of refraction can improve optical confinement as waveguide. The optical and electric properties of the thin films made by sol-gel process can be modulated according to the desired application. **Figure 6** shows transmittance curves of TiO_2 thin films deposited on glass substrates as a function of the number of layers. Each layer measures approximately 60 nm.

By these spectra it is possible to calculate the bandgap of the films using, for example, the Tauc method. The value measured in this case was 3.4 eV, meaning that the photocatalytic activity occurs at a wavelength in the UV region. Several studies are made aiming to reduce

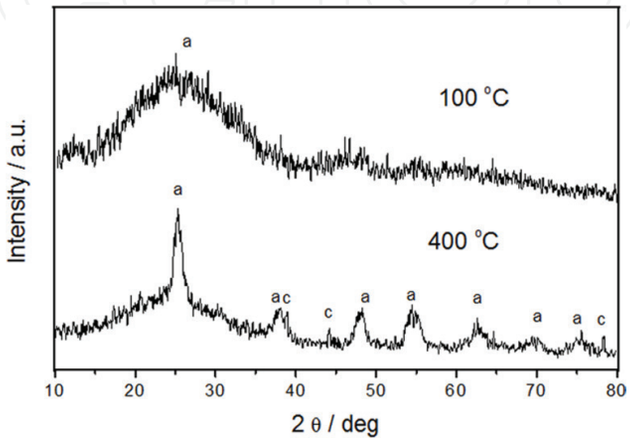

Figure 4. XRD patterns of TiO_2 thin films heated at (a) 100°C and (b) 400°C.

http://dx.doi.org/10.5772/intechopen.74335

the bandgap of the TiO_2 anatase phase to the visible region to make it a competitive energy source with application in photocatalysis, solar cells, and artificial photosynthesis.

TiO_2 films are also used in the preparation of hydrophobic and self-cleaning surfaces in several substrates. **Figure 7** shows water drops over the film surface and over the glass substrate surface. The contact angle can be change varying the film porosity and the number of layers, for example.

The TiO_2 self-cleaning surfaces have the ability to remove greasy dirt and bacteria from their surfaces due to their photocatalytic property, which promotes the breakdown of fat molecules or destroys the membranes of bacteria. The self-cleaning property is frequently connected to hydrophobic surfaces, because the dusts can be removed by the rolling of the water droplets in the surface.

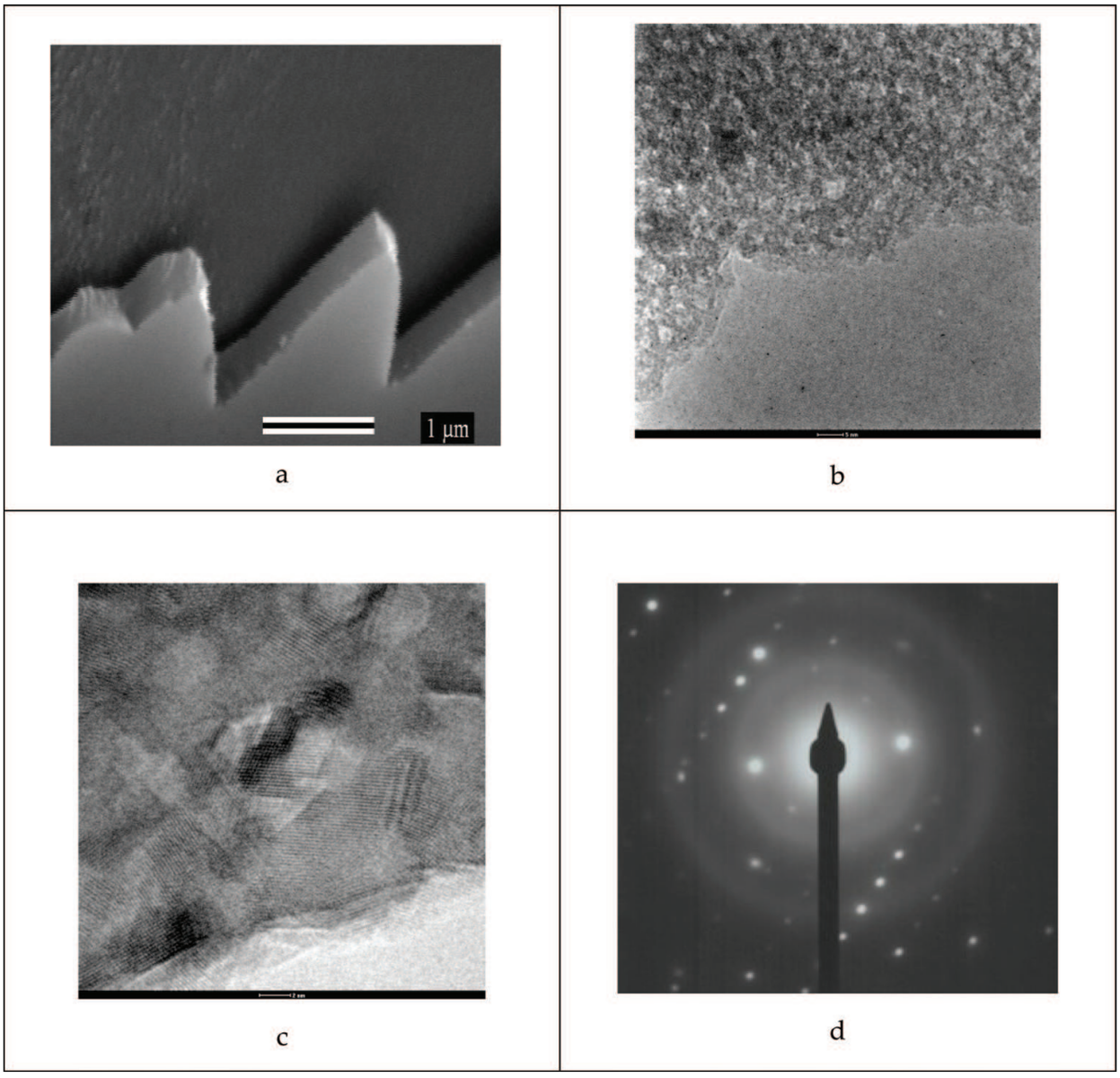

Figure 5. TiO_2 thin film images: (a) SEM image of the film over a glass substrate, (b) and (c) TEM images of the film, and (d) electron diffraction of the film.

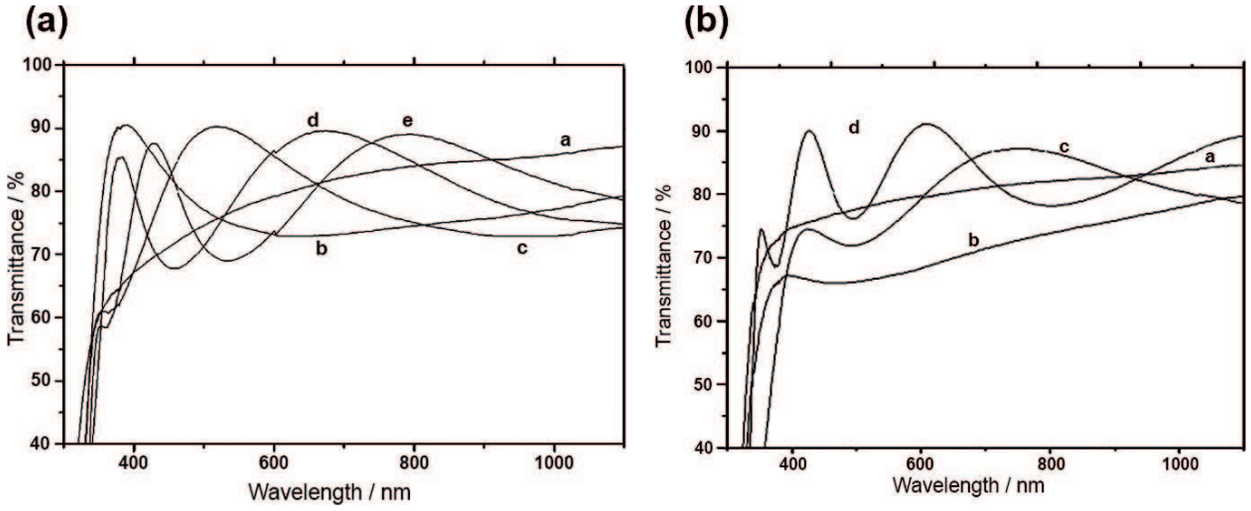

Figure 6. UV–Vis spectra of the films deposited on (a) both sides of a glass substrate and heated at 100°C: (a) glass, (b) one layer, (c) two layers, (d) three layers, (e) four layers, (f) five layers; (b) one side of the glass substrate and heated at 400°C: (a) one layer, (b) two layers, (c) three layers, and (d) five layers.

Figure 7. TiO_2 thin film deposited on (a) the film surface and on (b) the glass surface.

3. SiO_2/TiO_2 thin films

When Si alkoxide is mixed with Ti alkoxide to the preparation of precursors of TiO_2/SiO_2 thin films for utilization of the sol-gel process, the nanocomposites produced can combine or enhance the properties of the well-known pure oxides: TiO_2 and SiO_2 [6]. These nanomaterials can offer enhanced photocatalytic activities, persistent superhydrophilicity, modulated refractive index, enhanced resistance to corrosion, and superior mechanical properties such as larger mechanical resistance and hardness. The deposition of TiO_2/SiO_2 thin films in different substrates such as glasses, metals, ceramics, and polymers enables the application of these films in many purposes such as self-cleaning surfaces, antireflection surfaces, anticorrosion protection, wear resistance protection, fungicide and bactericide surfaces, water and air treatment devices, planar waveguides, nonlinear optical devices, etc. The most important fact is that two or more of these applications can be combined in TiO_2/SiO_2 multifunctional surfaces [7, 8].

In this work, the preparation of TiO_2/SiO_2 nanocomposite thin films was made using titanium isopropoxide (Aldrich, purity >98%), isopropyl alcohol and hydrochloric acid, to prepare the TiO_2 precursor solution and tetraethyl orthosilicate (Aldrich, purity >98%), isopropyl alcohol,

http://dx.doi.org/10.5772/intechopen.74335

hydrochloric acid, and distilled water to prepare the SiO_2 precursor solution. The pH of both solutions was maintained in 3. SiO_2 precursor solution was refluxed for 24 h at 60°C. Both the prepared solutions were aged for 24 h before the mixture. Then, TiO_2/SiO_2 precursor solutions

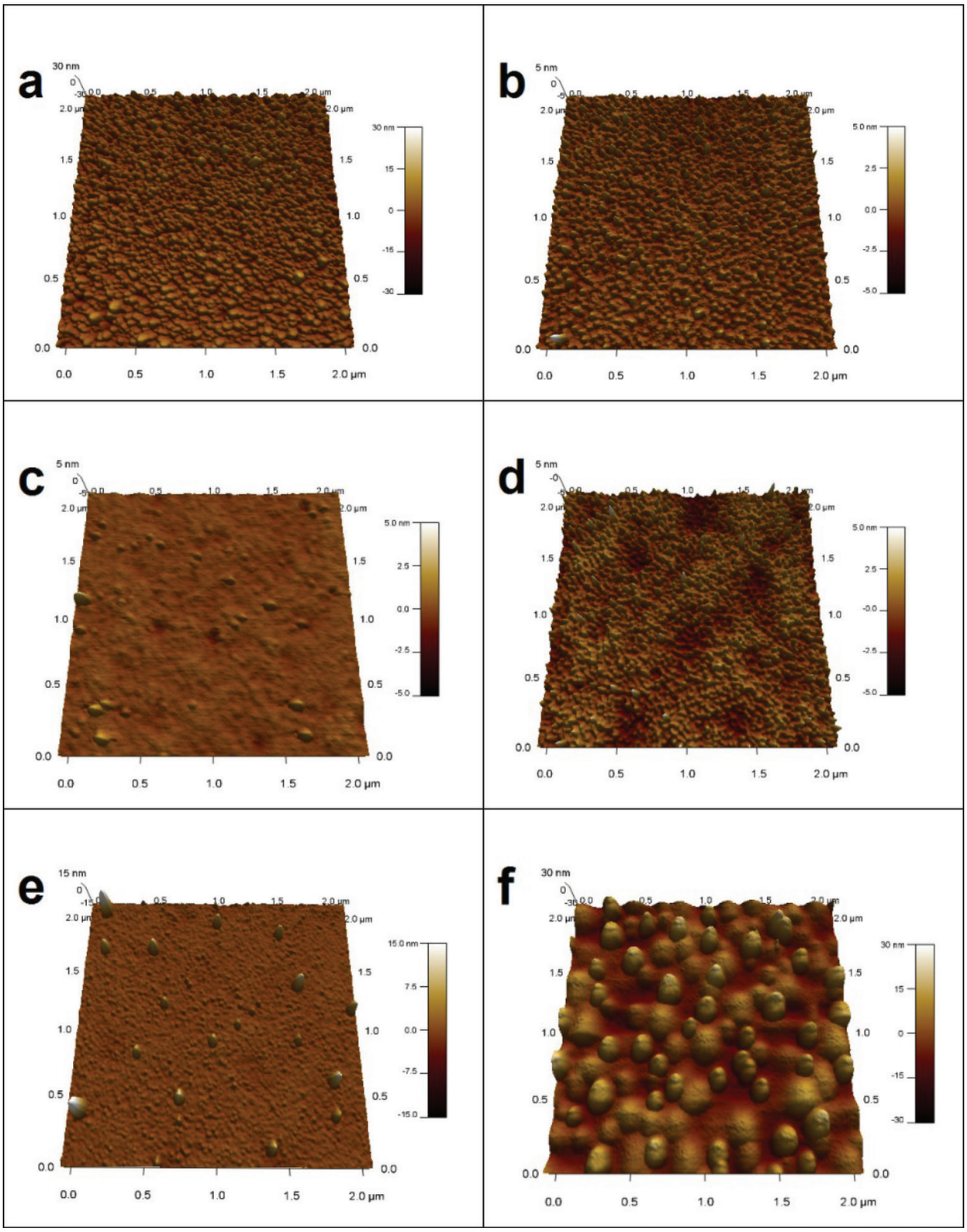

Figure 8. 3D topographies of the five-layer $xTiO_2/(100\text{-}x)SiO_2$ films: (a) TiO_2, (b) $Si_{20}Ti_{80}$, (c) $Si_{40}Ti_{60}$, (d) $Si_{60}Ti_{40}$, (e) $Si_{80}Ti_{20}$, and (f) SiO_2.

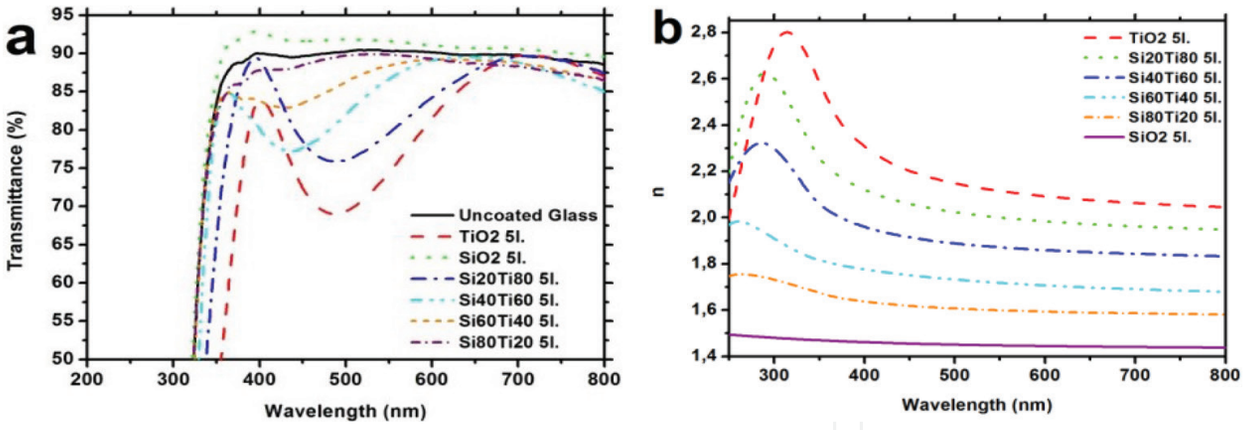

Figure 9. Optical properties modulation of the $xTiO_2/(100\text{-}x)SiO_2$ films: (a) transmittance and (b) refractive index in the function of wavelength.

with different $xTiO_2/(100\text{-}x)SiO_2$ molar ratios (x = 0, 20, 40, 60, 80, and 100%) were prepared and stirred for 1 h. The final viscosity of the solutions was maintained in approximately 2.2 cP. The films were deposited on properly clean glass substrates with a constant withdraw speed of 1.0 mm/s at 25°C and relative air humidity about 30%. The drying process occurred at 80°C in air for 10 min. This stage (deposition and drying) was repeated five times for thickness control. Finally, the samples were thermally treated at 500°C for 1 h.

The TiO_2 thin films were formed by anatase phase, and the SiO_2 thin films were amorphous according to XRD patterns and Raman spectroscopy results. The TiO_2/SiO_2 thin films are formed by the anatase phase dispersed in a vitreous matrix. The anatase phase is fundamental for the desired applications due to their optical and photocatalytic property. The microstructure, morphology, and texture of the $xTiO_2/(100\text{-}x)SiO_2$ thin films change substantially due to the mixture of the titanium and silicon oxide, as seen in AFM images of **Figure 8**.

With the addition of SiO_2, the titania nanoparticles remain dispersed in the vitreous matrix, and because of that, TiO_2 and SiO_2 pure films have higher root-mean-square (RMS) roughness (2.2 and 6.0 nm, respectively) than TiO_2/SiO_2 films (between 0.2 and 1.2 nm). The surface smoothing, after the mixture of TiO_2 and SiO_2, resulted in an enhanced hardness that changes to 4.5 GPa for both pure films and to approximately 7.4 GPa for all nanocomposite thin films. These properties are essential for outdoor applications, special windows, glasses of cars, and other vehicles, among others, since the film surfaces can be subjected to intense mechanical wear of air particles. Moreover, TiO_2/SiO_2 nanocomposite thin films present a persistent superhydrophilicity, which is required for application on self-cleaning surfaces and water/air treatment, promoting a better washing of the contaminants in the surface, which can be obtained with the rain precipitation. These nanocomposites increase the adsorption of pollutants by the surface.

The optical properties of the $xTiO_2/(100\text{-}x)SiO_2$ films are modulated by Ti/Si rate variation, as seen in **Figure 9**.

The possibility to modulate the transmittance and refractive index (n) of the $xTiO_2/(100\text{-}x)SiO_2$ thin films is essential in applications as antireflection surfaces, filters, and planar waveguides, since this wide variation of n (from 1.45 to 2.18 in visible light) permits the

http://dx.doi.org/10.5772/intechopen.74335

construction of different structural models of devices. The variation in the refraction index in function of incident light wavelength of 2.0–2.8 (**Figure 9b**) is also very important to the construction of nonlinear optic devices [9].

4. Ag/TiO_2 thin films

TiO_2 exhibits a high energy bandgap (3.2–3.8 eV) which corresponds to UV irradiation with a wavelength smaller than 388 nm. To overcome this limitation, several studies have been performed showing the modification of TiO_2 with metal and nonmetal species aiming to extend the light absorption to the visible range and simultaneously increasing the recombination time of the electron-hole pairs formed. In particular, nanocomposite thin films of silver and titania have been of considerable interest since silver nanoparticles can act as electron traps, contributing to electron-hole separation and creating a local electric field capable of facilitating the electron excitation and consequently their photocatalytic properties. The improvement in the photocatalytic properties leads to surfaces with better bactericide, hydrophobicity, and self-cleaning characteristics [10].

Ag/TiO_2 coatings were prepared from alcoholic solution containing titanium isopropoxide and silver nitrate dissolved in a mixture of isopropyl alcohol in several atomic ratios. Acid conditions (pH = 4) were reached after acetic acid addition. This precursor solution was stirred at room temperature during 1 h and submitted to UV-C irradiation (254 nm) treatment in air for 100 min. This procedure has been used to produce metallic Ag from Ag^+ ions. The films were deposited onto clean substrates as borosilicate, silicon, 316 L stainless steel, and magnets (NdFeB) with withdrawal speed of 8 mm s^{-1}. After deposition, the coatings with one to five layers were dried in air for 20 min and were thermally treated for 1 h between 100 and 400°C [5, 11].

Figure 10 shows the characteristic diffractogram of Ag/TiO_2 thin films with five layers deposited on glass and heated at 400°C.

According to XRD patterns, the coatings heated at 400°C show indexed peak characteristic of crystalline metallic Ag and anatase phase (PDF #1-562). The diffractogram of the film heated at 100°C was characteristic of a noncrystalline material, as expected. The substrates of 316 L stainless steel and magnets showed similar XRD patterns. SEM images of Ag/TiO_2 heated at 400°C deposited on different substrates are shown in **Figure 11**.

The structure of the used substrates has induced the formation of nano- and microstructures of metallic silver with different sizes and morphologies supported on the TiO_2 thin film surfaces. This formation occurs due to thermal treatment that induces the diffusion of the metal nanoparticles to the film surface. In the borosilicate substrate (**Figure 11a**), the formation of spherical Ag nanoparticles with a bimodal particle size distribution is observed. When substrates of 316 L stainless steel and magnets (NdFeB) were used, Ag dendrite micro- and nanostructures were formed (**Figure 11b** and **c**). A trimodal size distribution is observed for the particles present on the surface of the Ag/TiO_2 film deposited on silicon (**Figure 11d**). Particularly in this film, the Ag particles show dimensions of 5–150 nm.

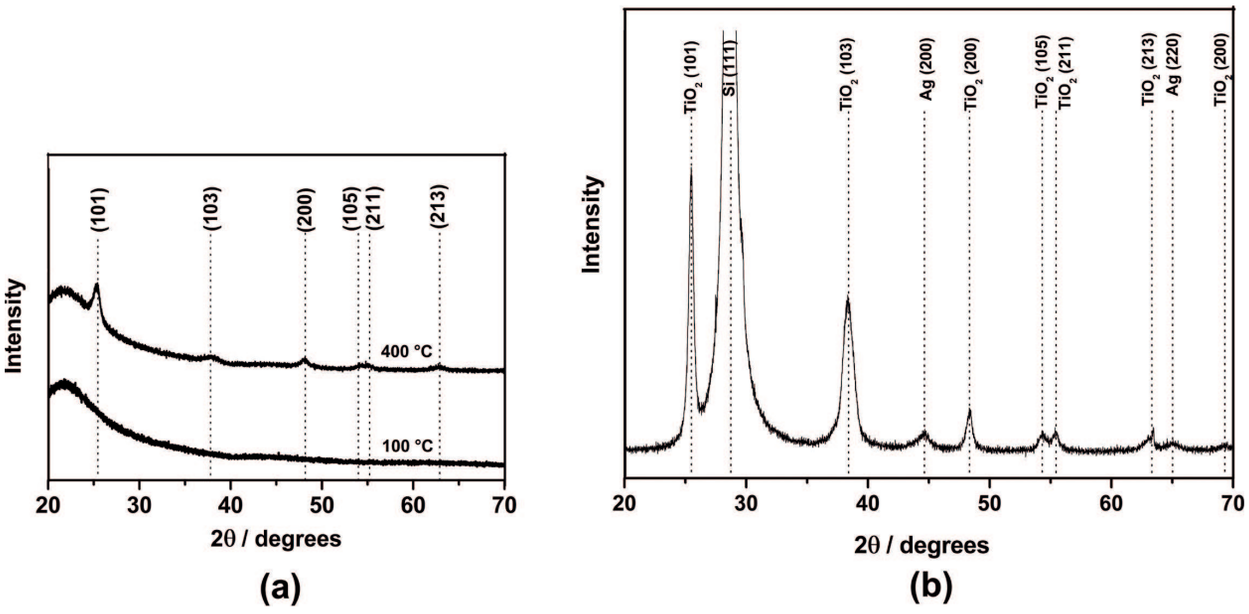

Figure 10. XRD patterns of Ag/TiO_2 thin films with five layers heated at 100°C and 400°C and deposited on (a) borosilicate and (b) silicon substrates (400°C).

Energy-dispersive spectra (EDS) shown in **Figure 12** has confirmed the elemental composition of the Ag/TiO_2 films treated at 400°C deposited on 316 L stainless steel. In this film's circular, micrometric and submicrometric structures also are observed besides the dendrites mentioned above. Brightness regions on the micrograph are constituted only by Ag, while the other regions are formed by TiO_2 matrix in the anatase phase, according to the XRD results. The analyses for the other substrates were similar.

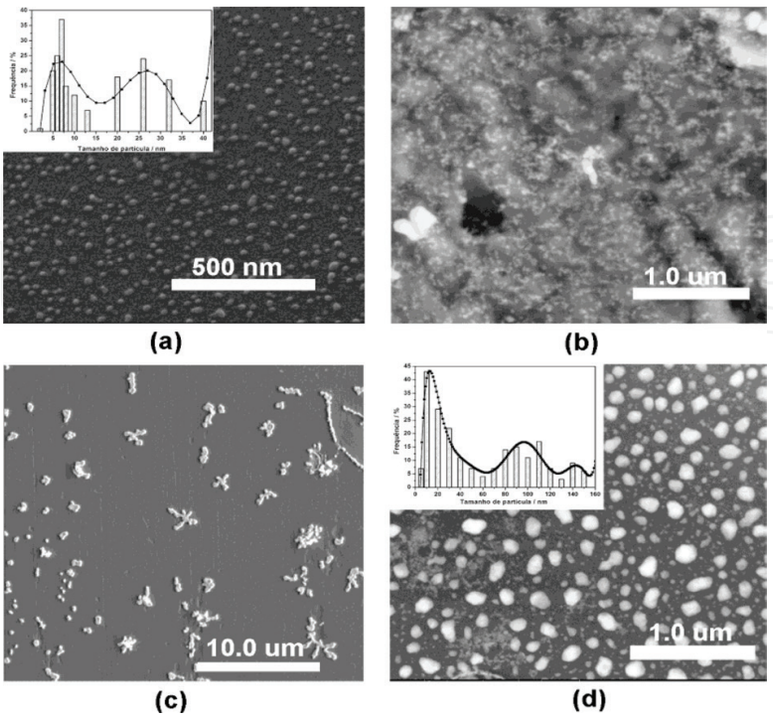

Figure 11. SEM images of Ag/TiO_2 heated at 400°C and deposited on (a) borosilicate, (b) magnet, (c) 316 L stainless steel, and (d) silicon substrates.

http://dx.doi.org/10.5772/intechopen.74335

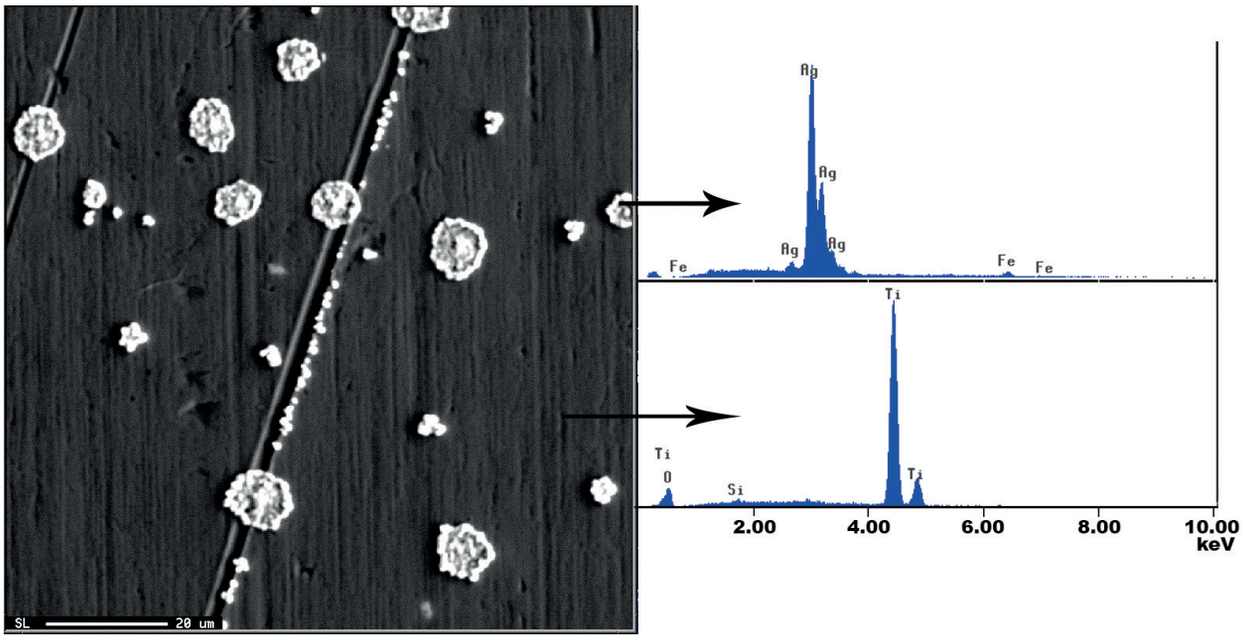

Figure 12. SEM-EDS of Ag/TiO_2 thin film heated at 400°C and deposited on 316 L stainless steel and EDS spectra from different regions in the surface.

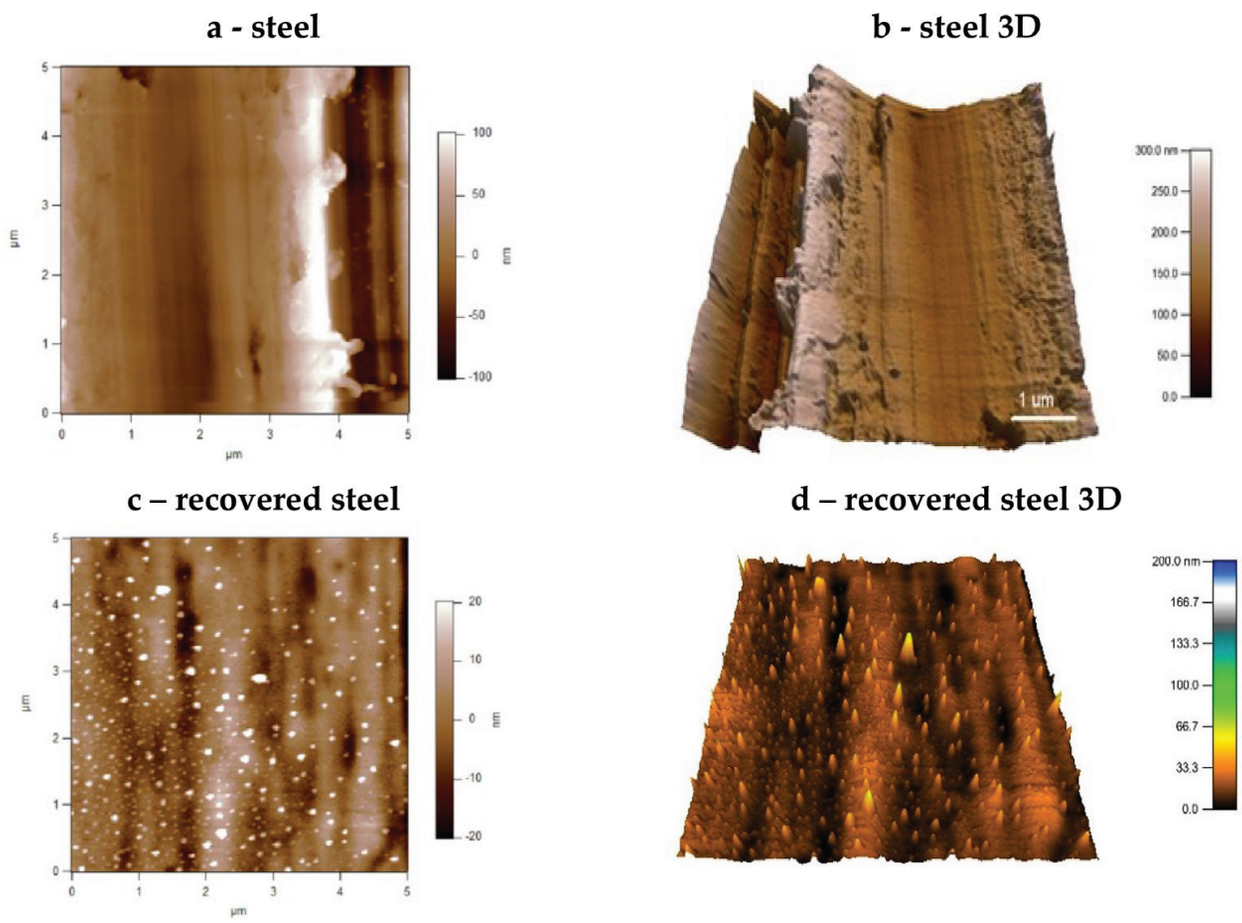

Figure 13. AFM images of (a and b) 316 L stainless steel and (c and d) Ag/TiO_2 thin film deposited on 316 L stainless steel and heated at 400° C (one layer).

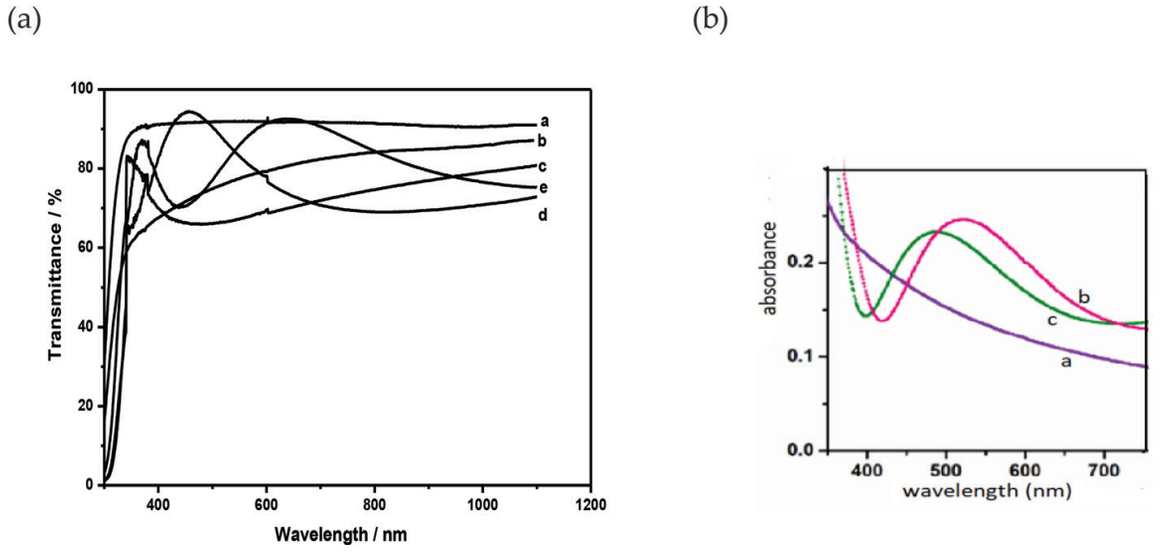

Figure 14. (a) Ag/TiO_2 thin film transmittance in the function of wavelength: (a) glass, (b) one layer, (c) two layers, (d) three layers, and (e) four layers. (b) Absorption spectra of (a) TiO_2; (b) Ag/TiO_2, Ag:Ti = 1:6; and (c) Ag/TiO_2, Ag:Ti = 1:100.

Figure 13 shows AFM images of Ag/TiO_2 thin films with one layer deposited on 316 L stainless steel substrate. The surface roughness of the 316 L stainless steel, whose texture is shown in **Figure 13a** and **b**, is ~40 nm, a much higher value compared to the roughness value of the borosilicate substrate, which is about 0.20 nm. It is observed that the Ag/TiO_2 films deposited on the steel substrates reduce their roughness as a function of the number of layers deposited. With four layers, the roughness value decreases to 7 nm. In addition, the Ag/TiO_2 films are formed by silver nanoparticles dispersed on the surface of the TiO_2 matrix with sizes between 20 and 50 nm.

The introduction of silver in the TiO_2 structure changes their optic properties as can be seen in **Figure 14a**, represented by the variation of transmittance in the function of wavelength. The bandgap decreases, depending on the amount of silver in the crystalline structure (Tauc method), until values of 1.75 eV depend on the concentration of silver, according to the literature [9].

Figure 14b shows the absorption spectra of pure and doped TiO_2, emphasizing the photonic property of the Ag/TiO_2 thin films, with absorption peaks between 490 and 520 nm that changed with the variation of the molar ratio (Ag:Ti). These photonic surfaces provide new possibilities to increase the efficiency of solar energy conversion by confinement of the light, improve bandgap effects, and enhance optical transmission as well as nonlinear optical switching in surface polaritonic structures.

Other utilizations of Ag/TiO_2 thin films are in hydrophilic/hydrophobic surfaces and in bactericide and fungicide devices [5], since the silver increases the TiO_2 efficiency.

5. Nb/TiO_2 thin films

Traditionally, the niobium is used mainly in the confection of metallic alloys for several industrial applications [12]. However, the use of niobium to produce ceramic materials is increasing in the last few years with several applications into catalysis, supercapacitor, and battery components, among others. The incorporation of the niobium in other material structures, causing

http://dx.doi.org/10.5772/intechopen.74335

substitutional defects, has been studied to improve several material properties, such as TiO_2. Examples of applications of Nb-doped TiO_2 are its use as photocatalyst, dye-sensitized solar cells, gas sensors, magnetic properties, and transparent conductive oxide (TCO) for several electronic devices.

Several methods are being used to synthesize and deposit Nb-doped TiO_2 thin films in different types of substrates. However, the most used deposition methods are chemical vapor deposition (CVD), sputtering, and sol-gel process. In the sol-gel synthesis of Nb-doped TiO_2, the use of mainly two niobium precursors, niobium ethoxide [$Nb(OCH_2CH_3)_5$], and niobium pentachloride ($NbCl_5$) that are very expensive is reported in the literature [13]. In this work, Nb/TiO_2 coatings were prepared from alcoholic solution containing titanium isopropoxide and ammonium-(bisaquo oxobisoxalato) niobate-trihydrate (produced by CBMM, Brazil) dissolved in a mixture of isopropyl alcohol. Acid conditions (pH = 4) were reached after acetic acid addition. The precursor solution was stirred at room temperature during 1 hour and deposited by dip-coating process in clean glass substrates with withdrawal speed between 0.8 and 3.7 mm s^{-1}. After deposition, the coatings with one to five layers were dried in air for 20 min and were thermally treated for 1 h between 100 and 500°C.

The $Nb\text{-}TiO_2$ thin films obtained are transparent, adherent, free of micro-cracks, and with visual appearance more homogeneous than the other deposited thin films. The niobium increases the mechanical resistance of the surface.

A theoretical study using density functional theory (DFT) showed that the insertion of niobium in the titanium dioxide matrix, causing the substitution of Ti^{4+} cations for Nb^{5+} cations, changes its lattice parameters, cell volume, and bandgap [14]. Therefore, the structures of the materials calcined at 500°C were found to be crystalline in the anatase phase (PDF #1-562). The thin films doped with 0.5, 1, and 3% molar ratio Nb:Ti showed a displacement of the 101 and 200 peaks to lower angles, evidencing the substitution of the niobium inside the crystal structure, as shown in **Figure 15**.

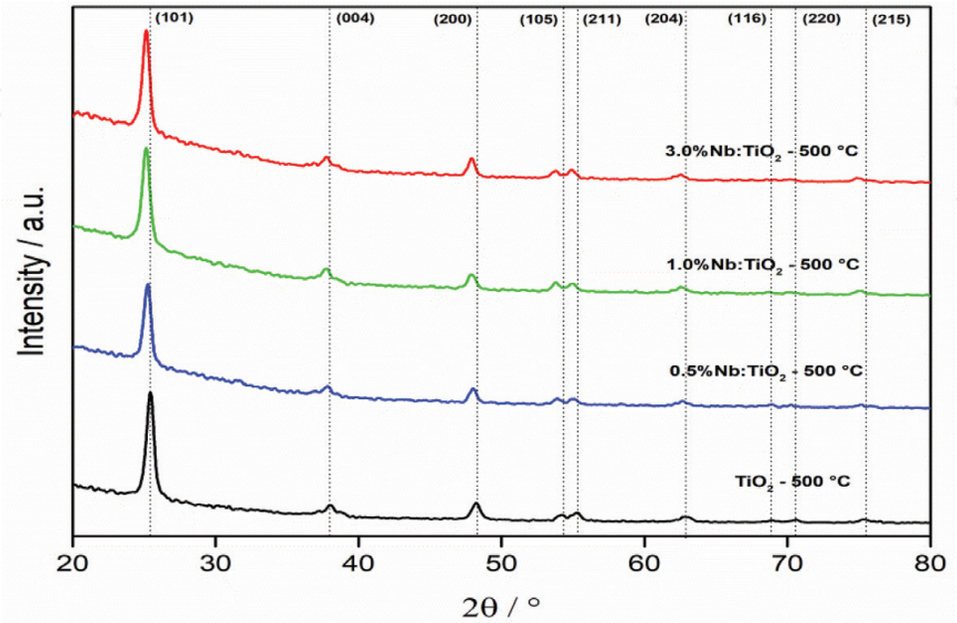

Figure 15. XRD patterns of TiO_2 thin films with different niobium concentrations, calcined at 500°C.

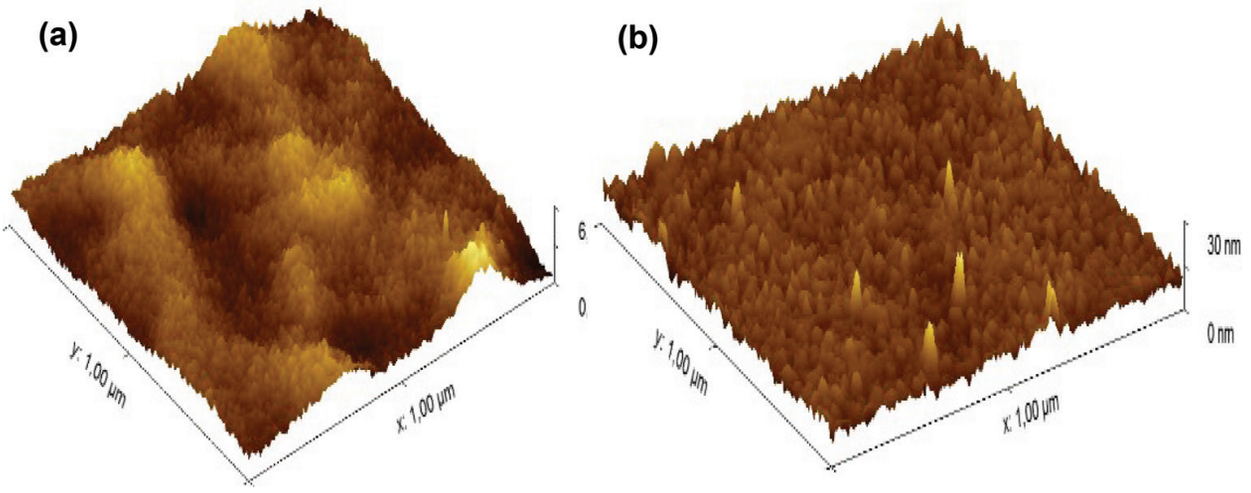

Figure 16. 3D micrographs of (a) 2% Nb-doped TiO_2 and (b) pure TiO_2, calcined at 500°C.

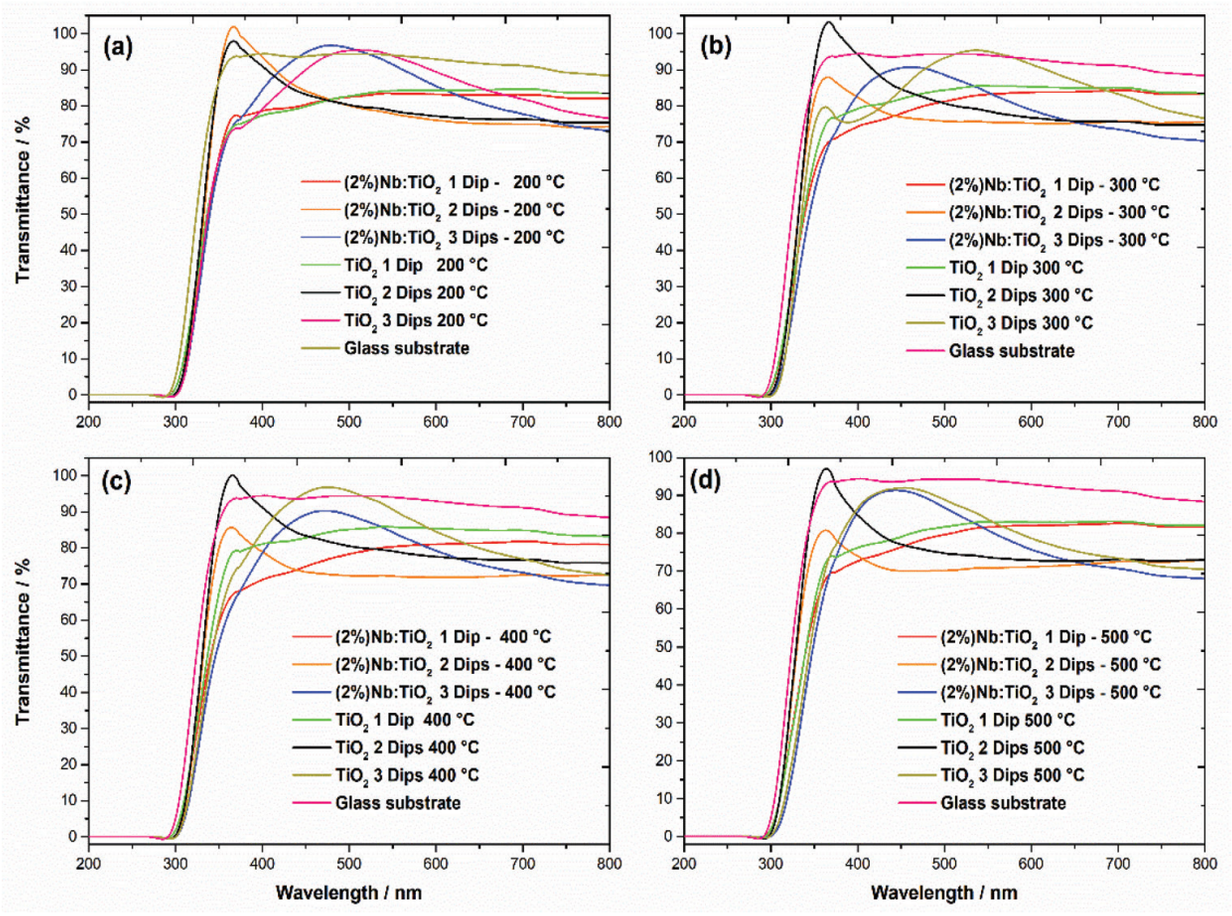

Figure 17. UV-Vis spectra of several TiO_2 and Nb/TiO_2 thin films with different calcination temperatures and numbers of layers.

The increase of niobium content in the thin film promoted a considerable variation in the lattice parameters, whose d_{101} changed to 3.49 for pure TiO_2 and to 3.55 for 3% Nb/TiO_2. The crystallite size decreased from 11 to 7 nm, which agreed with the DFT results previously reported.

http://dx.doi.org/10.5772/intechopen.74335

AFM 3D micrographs (**Figure 16a** and **b**) show that the TiO_2 has larger particle size and RMS roughness of 2.2 ± 0.1 nm, while the 2% Nb/TiO_2 film presents a RMS roughness of 0.6 ± 0.2 nm and smaller nanoparticles. All Nb/TiO_2 thin films presented different profiles than TiO_2 thin films, with smaller nanoparticles and RMS roughness and, therefore, more homogeneity, adherence, and visual quality.

UV-Vis spectra seen in **Figure 17** show that also it is possible to modulate the transmittance of the thin films as a function of the wavelength to obtain optical filters. All studied films showed similar bandgap values obtained by the Tauc method, between 3.6 and 3.4 eV. The insertion of niobium on the TiO_2 structure led to a denser film with higher refractive index and high mechanical resistance.

6. Conclusion

The sol-gel deposition parameters such as the density of the precursor solution, concentration of oxides, viscosity, withdrawal velocity, number of dips, and drying temperature influence the characteristics of the films such as thickness, porosity, refractive index, particle size, particle shape, and oxidation degree. Someway, all dopants used improved the quality and the range of application of the TiO_2 films. The addition of SiO_2 in the TiO_2 films changes their mechanical, optical, and surface properties. The addition of Ag increases its photocatalytic activity, improving fungicide and bactericide properties of the films. The hydrophobicity/hydrophilicity change capacity was improved too. The doping with Nb improves the mechanical resistance of the films. All these properties can be applied in the confection of best photocatalytic surfaces to be used in the production of solar energy, self-cleaning surface, and optical and nonlinear optical devices.

Acknowledgements

The authors would like to thank FAPEMIG, CNPq, and CAPES for their financial support and UFMG's Microscopy Center for the images.

Author details

Nelcy Della Santina Mohallem[1,2]*, Marcelo Machado Viana[1],
Magnum Augusto Moraes Lopes de Jesus[1], Gustavo Henrique de Magalhães Gomes[1],
Luiz Fernando de Sousa Lima[1] and Ellen Denise Lopes Alves[2]

*Address all correspondence to: nelcy@ufmg.br

1 Laboratory of Nanostructured Materials, Universidade Federal de Minas Gerais, Belo Horizonte, Minas Gerais, Brazil

2 REDEMAT, MG, Brazil

References

[1] Khataee A, Mansoori GA. Nanostructured Titanium Dioxide Materials. World Scientific; 2012

[2] Viana MM, Mohallem TDS, Nascimento GLT, Mohallem NDS. Nanocrystalline titanium oxide thin films prepared by sol-gel process. Brazilian Journal of Physics. 2006;**36**:1081-1083

[3] Brinker CJ, Scherrer GW. Sol-Gel Science. San Diego: Academic Press; 1990

[4] Mohallem NDS. $BaTiO_3$ thin films prepared by dip-coating process. MRS Proceedings. 1994;**341**:379

[5] Silva AFR, Mohallem NDS, Viana MM. TiO_2 and silver/titanium dioxide thin films with self-cleaning properties. Advanced Materials Letters. 2017;**8**:444

[6] Mohallem NDS, Aegerter MA. Multilayer SiO_2 and TiO_2 coatings on glasses by the sol-gel process. Journal of Non-Crystalline Solids. 1988;**100**(1-3):526-530

[7] Glaubitt W, Lobmann P. Antireflective coatings prepared by sol–gel processing: Principles and applications. Journal of the European Ceramic Society. 2012;**32**(11):2995-2999

[8] Jesus MAML, da Silva JT, Timò G, Paiva PP, Dantas MS, Ferreira AM. Superhydrophilic self-cleaning surfaces based on TiO_2 and TiO_2/SiO_2 composite films for photovoltaic module cover glass. Applied Adhesion Science. 2015;**3**(1):1-9

[9] Hari M, Joseph SA, Mathew S, Radhakrishnan P, Nampoori VPN. Band-gap tuning and nonlinear optical characterization of Ag:TiO_2 nanocomposites. Journal of Applied Physics. 2012;**112**:074307

[10] Viana MM, Mohallem NDS, Miquita DR, Balzuweit K, Silva-Pinto E. Preparation of amorphous and crystalline Ag/TiO_2 nanocomposite thin films. Applied Surface Science. 2013;**265**:130

[11] Yadav S, Jaiswar G. Review on undoped/doped TiO_2 nanomaterial; synthesis and photocatalytic and antimicrobial activity. Journal of the Chinese Chemical Society. 2017;**64**:103-116

[12] Wen M, Wen C, Hodgson P, Li Y. Fabrication of Ti–Nb–Ag alloy via powder metallurgy for biomedical applications. Materials & Design (1980-2015). 2014;**56**:629-634

[13] Bakhshayesh AM, Bakhshayesh N. Improved short-circuit current density of dye-sensitized solar cells aided by Sr, Nb co-doped TiO_2 spherical particles derived from sol-gel route. Journal of Sol-Gel Science and Technology. 2016;**77**:228-239

[14] Kamisaka H, Hitosugi T, Suenaga T, Hasegawa T, Yamashita K. Density functional theory based first-principle calculation of Nb-doped anatase TiO_2 and its interactions with oxygen vacancies and interstitial oxygen. The Journal of Chemical Physics. 2009;**131**. https://doi.org/10.1063/1.3157283